Bulg. J. Phys. **37** (2010) 105–114

The Gaussian Absorption Damping Effects on ATIR

H. Stoyanov

Department of Quantum Electronics, Faculty of Physics, University of Sofia, 5, James Bourchier Blvd., Sofia 1164, Bulgaria

Received *27 May 2010*

Abstract. A simple shearing polarization interferometer was used to investigate the effect of the inhomogeneous distributed absorption in the gap formed by a glass prism and a metal attenuator on the complex amplitude of the reflected field. A perfect tree layered system is considered so that the gap can be regarded as a plane parallel micro cuvette. In our case this cuvette is filled with a liquid with Gaussian distribution of the extinction coefficient (the imaginary part of the complex index of refraction). From this follows a proportional variation of the optical thickness of the separation between the prism boundary and the attenuator face and specific distribution of the phase shift between the p- and s-components of the reflected field. The interferometer allows to separate these two components and to let them interfere [1]. The phase shift distribution along the aperture of the beam can be determined from the interference signal. An experiment with a glass prism-liquid-plane silicon attenuator is described. The results are compared with the theoretical predictions. For angles of incidence larger than the critical one a good agreement between theory and experiment was observed.

PACS number: 42.25.Fx, 42.25.Gy, 42.60.Jf

1 Introduction

The total internal reflection (TIR) phenomenon serves as a basis for great variety of useful applications. The attenuated TIR (ATIR) was initially used for creating fixed or variable phase retarders [2-4] and variable filters [5], in the optical refractometry of absorbing liquids [6-9], metals, biotissue [10], for study of the subwavelength surface relief [11], *etc.* A very important area of application of ATIR is the surface plasmon resonance effects [12] and their applications in material science [13]. The classical ATIR configuration is a perfect three layered system with two parallel plane boundaries. All media are expected to be homogeneous. In contrary any deviation from this model leads to nontraditional effects.

In the present paper we study the reflected optical field in the situation of intermediate space filled with inhomogeneous liquid. In our model the distribution of the optical absorption in the gap has central symmetry and obeys the Gaussian law. In addition, a recently described method [14] based on the reduced Rayleigh integral equation allows us to study the ATIR reflected field in the case of curved attenuator what recalculated to the optical thickness allows to apply the same method. The present work demonstrates that for a system composed of almost plane boundaries the simpler Mueller matrix method gives sufficiently good results and also presents comparison between theory and experiment.

2 The Optical Setup

In the present work we are following the same way of studying of the process of TIR attenuation and the same optical setup as that described in [8]. The optical system used in the experiment is shown in Figure 1. The laser source L emits a linearly polarized beam which is expanded and collimated by the collimator K. The obtained plane wave propagates through the TIR prism *PR*. The glass prism and the attenuator are mounted on a precise rotating stage. The polarization beam splitter R followed by the linear polarizer Pol, compose a simple shearing interferometer which allows us to study the phase shifts between the basic polarization components and their amplitude changes as well. The interferometric fringes are detected by a linear array image sensor *Det* and analyzed by a PC-AT compatible computer. All elements are mounted on a vibration isolated optical table.

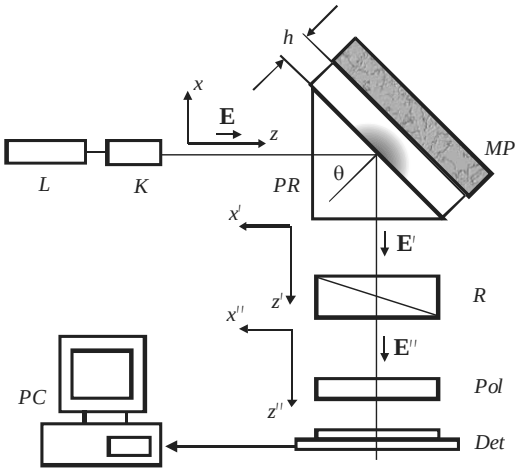

Figure 1. Sketch of the equipment: L – laser source; K – collimator; *PR* – glass prism; *MP* – metal plate; R – Rochon prism; *Pol* – linear polarizer; *Det* – photodiode array detector; *PC* – personal computer with a framegraber.

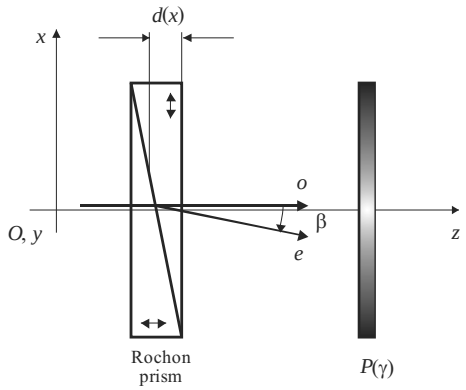

Figure 2. Sketch of the shearing interferometer.

Following the classical way [17] of studying of the process of TIR we regard the incident and the output fields as compositions of two independent fields: the p- and s-polarized components. A meridional view of the interferometer is shown in Figure 2. It is a common path polarization shearing interferometer. The coordinate system is oriented so that the z axis is along the direction of propagation of the laser beam and the x axis is in the plane of incidence. The field vector $\boldsymbol{E}$ in the entrance pupil of the optical system (the TIR prism with the metal plate *MP* acting as attenuator) subtends an azimuthal angle σ with the plane of incidence. The exit pupil of the electric field $\boldsymbol{E}'$, represented by its Jones vector, is given by [17]

$$\begin{bmatrix} E'_p \\ E'_s \end{bmatrix} = \begin{bmatrix} r_p & 0 \\ 0 & r_s \end{bmatrix} \begin{bmatrix} E_p \\ E_s \end{bmatrix} , \tag{1}$$

where $E_p = |\boldsymbol{E}| \cos\sigma$ and $E_s = |\boldsymbol{E}| \sin\sigma$ are the components of the entrance Jones vector (for the p- and s-polarization, respectively). The complex amplitude reflection coefficients are written as

$$r_p = \rho_p \exp(i\delta_p) , \qquad r_s = \rho_s \exp(i\delta_s) . \tag{2}$$

The phase difference between the two components we denote by $\Delta = \delta_p - \delta_s$. This quantity can be determined out by analyzing the fringe pattern at the exit of the interferometer. The expressions for calculating r_p and r_s, derived on the basis of the theory of stratified optical media are [17,19]

$$r_s = \frac{Z^i_{0s}(A - CZ^f_{0s}) + (B - AZ^f_{0s})}{Z^i_{0s}(A + CZ^f_{0s}) + (B + AZ^f_{0s})} , \tag{3}$$

$$r_p = \frac{Z^i_{0p}(CZ^f_{0p} - A) + (AZ^f_{op} - B)}{Z^i_{0p}(CZ^f_{0p} + A) + (AZ^f_{0p} + B)} , \tag{4}$$

where the indices i and f refer to the initial and final media, respectively. A, B, C are the elements of the transmission matrix through the gap with thickness h

$$\begin{bmatrix} A & B \\ C & D \end{bmatrix} = \begin{bmatrix} \cosh \alpha_2 h & Z_{0,2} \sinh \alpha_2 h \\ Z_{0,2}^{-1} \sinh \alpha_2 h & \cosh \alpha_2 h \end{bmatrix}, \tag{5}$$

where

$$\alpha_2 = k\Big[\Big(\frac{n_3}{n_2}\Big)^2 \sin^2 \theta_3 - 1\Big]^{1/2}.$$

The characteristic boundary impedance $Z_{0,2}$ is given by

$$\begin{aligned} Z_{0,2} &= (n_2 \cos \theta_2)^{-1} \qquad \text{for } s\text{-polarization, and} \\ Z_{0,2} &= n_2^{-1} \cos \theta_2 \qquad \text{for } p\text{-polarization,} \end{aligned} \tag{6}$$

where

$$\cos \theta_2 = -i\Big[\Big(\frac{n_3}{n_2}\Big)^2 \sin^2 \theta_3 - 1\Big]^{1/2}$$

gives the direction of propagation of the wave in the second medium (in our case liquid). The characteristic boundary impedances of the initial and final media for both p- and s-component of the field are given, respectively by

$$Z_{0,s}^i = [(n_1 - i\kappa_1) \cos \theta_1]^{-1}, \qquad Z_{0,s}^f = (n_3 \cos \theta_3)^{-1}, \tag{7}$$

$$Z_{0,p}^i = (n_1 - i\kappa_1)^{-1} \cos \theta_1, \qquad Z_{0,p}^f = n_3^{-1} \cos \theta_3, \tag{8}$$

where $\sin \theta_1 = (n_3 \sin \theta_3)/(n_1 - i\kappa_1)$, $\cos \theta_1 = (1 - \sin^2 \theta_1)^{1/2}$, $\Re[\cos \theta_1] > 0$, n_3 is the index of refraction of the glass prism *PR* (see Figure 1). $\hat{n}_1 = n_1 - i\kappa_1$ is the complex index of refraction of the bulk absorbing medium *MP*. When the angle of incidence θ_3 exceeds slightly the critical angle of TIR, the complex amplitude coefficients (2) exhibit strong dependence on the boundary conditions. These conditions, (presented by the characteristic boundary impedances) are functions of the optical properties of all media. We suppose constant and homogeneous optical properties of the glass prism and the metal attenuator. In our experiment the intermediate space is filled with water solution of malachite green dye. A drop of the dye was added in the center of the prism hypotenuse face, Figure 2.

Here we suppose a quasi-static dynamics of the mixture of particles of dye in solvent. The particles are spheres of permittivity ε_i located randomly in a homogeneous environment ε_e and occupy a volume fraction f. The quasi-static nature of the mixture means that the wavelength of the optical field is much larger than the inclusion diameter. According to the Maxwell–Garnett mixing rule the mixture will have effective permittivity ε_{eff} given in [20]

$$\varepsilon_{\text{eff}} = \varepsilon_e + 2f\varepsilon_e \frac{\varepsilon_i - \varepsilon_e}{\varepsilon_i + \varepsilon_e - f(\varepsilon_i - \varepsilon_e)} \tag{9}$$

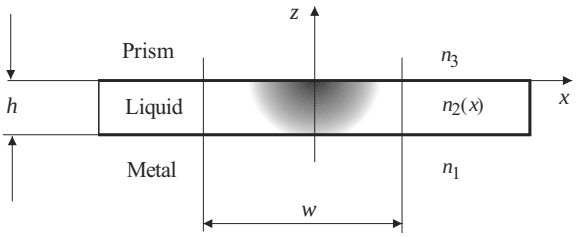

Figure 3. The geometry of the micro cuvette.

and the characteristic boundary impedances in the second medium (6) will be

$$Z = Z_0 \frac{1 + i\varepsilon_{\text{eff}}^{-1/2}\text{tg}(kw)}{1 + i\varepsilon_{\text{eff}}^{1/2}\text{tg}(kw)}\,, \tag{10}$$

where $Z_0 = \sqrt{\mu_0/\varepsilon_0}$ is the free space impedance, $k = (\omega/c_0)\varepsilon_{\text{eff}}^{1/2}$ is the wave number, ω is the angular frequency and c_0 is the velocity of light in a vacuum, w is the length of the irradiated area, Figure 3. In this case the Gaussian function [18] was assumed for the extinction and the index of refraction can be expressed in the form

$$n_2(x) = \sqrt{\varepsilon_{\text{eff}}} = n_0 - iN\exp(-\alpha x^2), \tag{11}$$

where n_0 and N are real constants, ε_{eff} is the effective permittivity of the liquid solution. Then the reflected field will be mainly dependent on the angle of incidence θ_3 and on the optical thickness $n_2(x)h$ of the gap.

If the detector, Figure 1, is a linear photodiode array oriented along the x axis, the measured fringe intensity distribution is [1]

$$I(x) = I_0\cos^2(\sigma)\cos^2(\gamma)\Big\{\rho_p^2 + \rho_s^2\text{tg}^2(\sigma)\text{tg}^2(\gamma) + 2\rho_p\rho_s\text{tg}(\sigma)\text{tg}(\gamma)\cos[\Phi(x,\Delta)]\Big\}. \tag{12}$$

The phase term $\Phi(x,\Delta)$ has the form

$$\Phi(x,\Delta) = (\boldsymbol{k}_p - \boldsymbol{k}_s)\cdot\boldsymbol{r} + \frac{2\pi}{\lambda}d(x)\Big[n_o - \frac{n_e(\beta)}{\cos(\beta)}\Big] + \Delta, \tag{13}$$

where $\Delta = \delta_p - \delta_s$ is the phase difference between both components, β is the angle deviation between the ordinary and the extraordinary rays at the exit of the Rochon prism (the angular shear), Figure 2, γ is the azimuth of the polarizer, measured from the plane of incidence O, x, z, $d(x)$ is the current thickness of the second right angle prism of the Rochon prism, $\boldsymbol{r}$ is the radius vector of the current point of measurement. In our case it lays in the plane of incidence O, x, z, $\boldsymbol{k}_p$, $\boldsymbol{k}_s$ are the wave vectors of the ordinary and extraordinary waves, which are

corresponding to the p- and s-components of the ATIR field, respectively, n_o, n_e are the ordinary and extraordinary refractive indices of the material, from which the Rochon prism has been fabricated.

The first two terms in Eq. (13) form the carrier frequency of the interferometric signal. For a plane wave this signal represents a family of straight parallel fringes. The third term ($\Delta = \delta_p - \delta_s$) in (13), which is a function of additional physical and geometric parameters, leads to distortion of the basic set of fringes provided that the azimuthal angles ε and γ are kept constant.

From the expressions for r_p and r_s it is clear that ρ_p, ρ_s and Δ depend on the complex optical thickness $\hat{n}_2(x)h$ of the micro cuvette (the gap), on the angle of incidence and on the optical properties of the media the light is passing through. The theoretical investigation of the h-dependence of ρ_p, ρ_s, [1], shows that it is not as strong and can be neglected in the first approximation. The interferometric signal, detected by the linear detector, is governed mainly by the phase difference Δ.

The numerical model of the Eq. (12) allows predicting the intensity distribution in the output interferometric signal along the axes of the linear sensor for various combinations of optical materials and for any polarization state of the incident wave. Even the case of inhomogeneous intermediate medium can be studied in this way. In Figure 4 we show the theoretical fringe intensity distribution along the aperture of the linear sensor as a function of the separation h (the thickness of the micro cuvette) between the TIR prism and the metal attenuator for the media used in the following experiment, silicon mono-crystal $\hat{n}_1 = 3.83 - i0.02$ [15], liquid $n_2(x)$, $n_3 = 1.56687$ Schott BaK4 glass. For comparison we carried out the same calculations for aluminum attenuator with index of refraction $\hat{n}_1 = 1.379 - i7.619$, [16], and the fringe intensity distribution is shown in Figure 5. Both examples were calculated for water basis of the liquid. In Figure 6 is shown the theoretical fringe intensity distribution for oil basis.

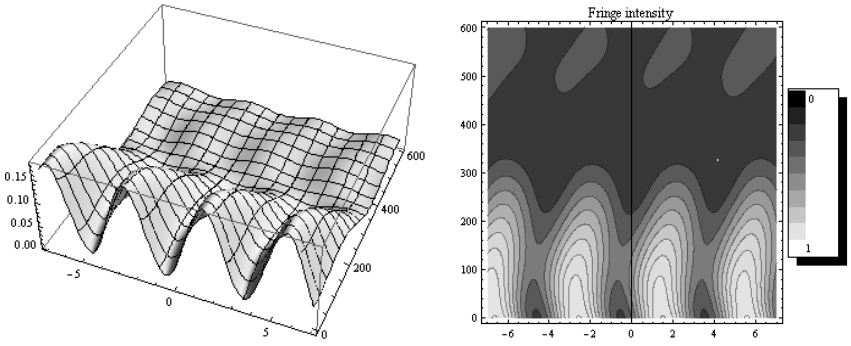

Figure 4. The theoretical fringe intensity distribution for silicon mono-crystal attenuator ($\hat{n}_1 = 3.85 - i0.02$ at $\lambda = 632.8$ nm [15]), $\hat{n}_2 = 1.33 - i0.1\exp[-x^2/300]$ (water), $n_3 = 1.56687$.

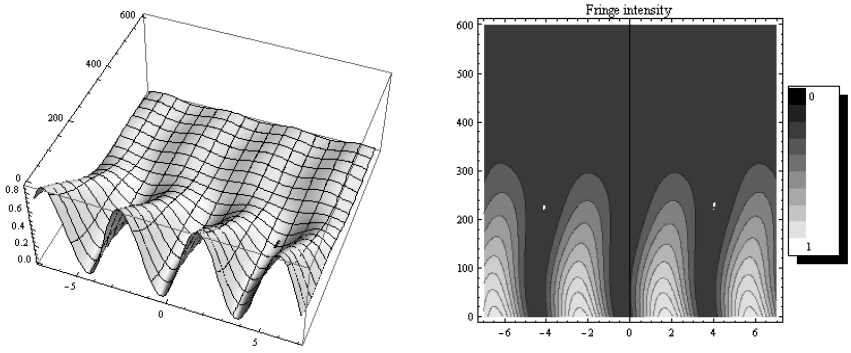

Figure 5. The theoretical fringe intensity distribution for aluminum attenuator $\hat{n}_1 = 1.379 - i7.619$ at $\lambda = 632.8$ nm [16], $\hat{n}_2 = 1.33 - i0.1\exp[-x^2/300]$ (water), $n_3 = 1.56687$.

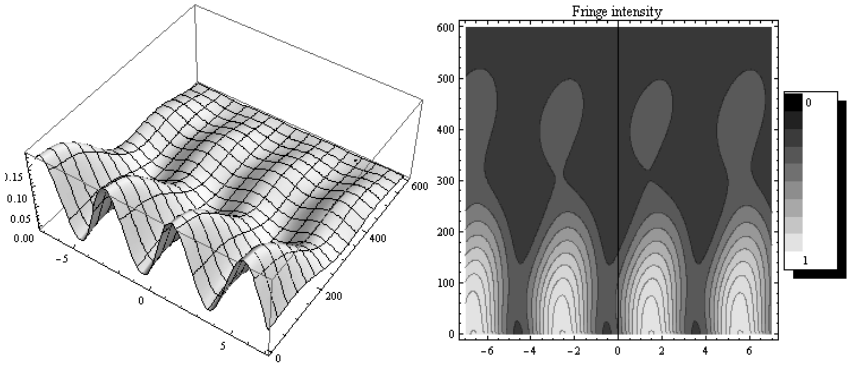

Figure 6. The theoretical fringe intensity distribution for silicon mono-crystal attenuator $\hat{n}_1 = 3.85 - i0.02$ at $\lambda = 632.8$ nm [15], $\hat{n}_2 = 1.43 - i0.1\exp[-x^2/300]$ (oil), $n_3 = 1.56687$.

3 Experimental Results and Discussion

The source of linearly polarized coherent light in Figure 1 is a HeNe laser (*Melles Griot*, 3 mW), working in TEM_{00} mode. The beam is expanded and collimated up to approximately 50 mm dia. by a well corrected collimator (*Jodon*, model BET–50). From the so generated plane wave only a small part was used – approximately 2×15 mm in the central area of the aperture. The prism *PR* was made of optical glass BaK4 (*Schott Jena*) with $n_3 = 1,56687$ at $\lambda = 632,8$ nm. The polarization interferometer consists of a Rochon prism and sheet linear polarizer. The Rochon prism provides an angular shear β of about 1.77×10^{-4} rad so that only approximately four fringes cover the full aperture of the sensor. The photodiode array image sensor (*Matsushita*, model

MN-512K) with 512 elements was used to detect photometric sections through the interferometric fringes. The sensor pixel dimensions are 28×16 μm and the pitch is 28 μm. The total length of the sensitive area is 14.3 mm. The ADC converter of the slot card framegraber provides 8 bits quantization of the video signal. Special attention has been paid to the determination of the gap thickness h. This measurement was carried out visually (in a manner similar to the described in [1]) by means of measuring microscope (not shown in Figure 1) with long working distance lens (about 122 mm). The white light Fizeau fringes were observed in direction approximately normal to the hypotenuse of the TIR prism. The tilt adjustment was accomplished by a three point micro screw adjusting stage mounted on the rotating table. From the initial situation the sample was translated step by step away from the prism and the movement of the dark brown-yellow fringe ($\lambda = 419$ nm approximately) was registered by the microscope. The wedge angle value between the prism hypotenuse and the metal surface was approximately 0.5×10^{-4} rad. The angle of incidence was measured and adjusted by a precise rotating stage (*Thorlabs*, Model 7R7) which offered resolution of 1 arc minute. An optically polished plate of silicon mono-crystal, N-type, cut at (1,0,0) ($\hat{n}_1 = 3.85 - i0.02$ at $\lambda = 632.8$ nm [15]) was used as attenuator.

The intermediate space was filled with oil. A tiny drop of malachite green dye was added in the central region of the micro cuvette formed in this manner. The array sensor allows us to capture and register almost linear photometric sections of the fringe intensity distribution shown in Figure 5. The results of the experi-

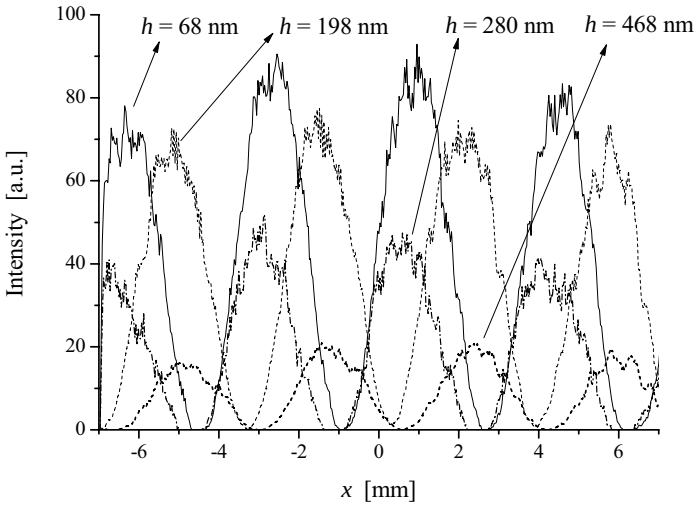

Figure 7. Photometric sections through the fringe intensity distribution for four different separations h.

ment in the form of four photometric sections are shown in Figure 7. For angles of incidence exceeding the critical one the interferometer forms approximately four full fringes in the input pupil of the sensor. As have been expected the presence of symmetrical distribution of the absorption leads to deformation and progressive one side shift of the fringes together with decreasing of the fringe visibility in the reflected field. The side fringe shift progressively increases for separation greater than $h = 150$ nm. And what is new, at $h \sim \lambda/2$ a phase jump is observed. This phenomenon requires further investigation. The experimental results shown in Figure 7 are in a quite good agreement with the numerically predicted intensity distribution for the situations when the intermediate space is filled with air.

4 Conclusion

The here described interferometer measurement proved to be a successful tool for ATIR phase investigation of absorbing liquids. The experiment gave results in good agreement with theory. The method can be used with success in the research and in other applications like the sensor technique, refractometry of absorbing media, contamination monitoring *etc*.

Acknowledgments

This work was supported by the National Science Fund of Bulgaria, grant No. DO-02-0114-2008 and grant No. DRNF-02/8-2009.

References

[1] H.Y. Stoyanov (2000) *Opt. Laser Technol.* **32** 147.
[2] A.M. Kan'an, R.M.A. (1994) *Opt. Eng.* **33** 2029.
[3] E. Cojocaru (1994) *Appl. Opt.* **33** 7425.
[4] E. Spiller (1984) *Appl. Opt.* **23** 3544.
[5] Y. Wang (1995) *Appl. Phys. Lett.* **67** 2759.
[6] W. Wild (1982) *Phys. Rev. A* **25** 2099.
[7] H.Y. Stoyanov (2006) *Bulg. J. Phys.* **33** 25.
[8] H.Y. Stoyanov (2007) *Opt. Laser Technol.* **39** 885.
[9] M. McClimans, C. LaPlante, D. Bonner, S. Bali (2006) *Appl. Opt.* **45** 6477.
[10] H. Li, S. Xie (1996) *Appl. Opt.* **35** 1793.
[11] J.C. Martinez-Anton (2006) *J. Opt. A Pure Appl. Opt.* **8** S213.
[12] V.M. Arganovich, D.L. Mills (1982) "*Surface Polaritons*", Elsevier, New York.
[13] D. Roy, J.H. Fendler (2004) *Adv. Mater.* **16** 479.
[14] Z.D. Genchev, H.Y. Stoyanov (2005) *Appl. Phys. B* **81** 657.
[15] R.M.A. Azzam (1985) *Appl. Opt.* **24** 513.

[16] M.J. Weber (2002) "*Handbook of Optical Materials"*, CRC Press, Boca Raton.

[17] W. Culshow (1972) *Appl. Opt.* **11** 2639.

[18] R. Escalona (2003) *J. Opt. A: Pure Appl. Opt.* **5** S355.

[19] Z. Knittl (1976) "*Optics of Thin Films*", John Wiley & Sons, Ltd. New York.

[20] K.K. Kärkkäinen, A.H. Sihvola, K.I. Nikoskinen (2000) *IEEE Trans. Geosci. Remote Sens.* **38** 1303.